Effect of quercetin on inhibiting gefitinib-activated non-small cell lung cancer-induced cell pyroptosis in cardiomyocytes via modulating mitochondrial autophagy mediated by the SHP2/ROS/AMPK/XBP-1/DJ-1 signaling pathway

JIE ZHANG[1], SHANSHAN QI[2], YANYAN DU[3], HONGHONG DAI[4] and NINGHUA LIU[5]

[1]Traditional Chinese Medicine Department, The Fourth Hospital of Hebei Medical University, Shijiazhuang, Hebei 050000, P.R. China;
[2]Department of Oncology, Shijiazhuang Hospital of Traditional Chinese Medicine, Shijiazhuang, Hebei 050000, P.R. China;
[3]Clinical Laboratory Department, The Fourth Hospital of Hebei Medical University, Shijiazhuang, Hebei 050000, P.R. China;
[4]Gynecology and Oncology Department, The Fourth Hospital of Hebei Medical University, Shijiazhuang, Hebei 050000, P.R. China;
[5]Functional Department, The Fourth Hospital of Hebei Medical University, Shijiazhuang, Hebei 050000, P.R. China

Received July 15, 2024; Accepted February 14, 2025

DOI: 10.3892/or.2025.8890

Abstract. It has been reported that treatment of patients with non-small cell lung cancer (NSCLC) with gefitinib increases the risk of QT interval prolongation. Therefore, the present study aimed to investigate whether quercetin could delay gefitinib-induced cardiomyocyte apoptosis and its underlying mechanism. A total of 32 nude mice were divided into the sham, NSCLC, NSCLC + gefitinib and NSCLC + gefitinib + quercetin groups. Cardiac fibrosis in mouse heart tissues was assessed by Masson's trichrome staining. Additionally, immunohistochemical staining was performed to detect the expression levels of Src homology-2 domain-containing protein tyrosine phosphatase (SHP2), X-box binding protein 1 (XBP-1), phosphorylated (p)-stimulator of interferon genes (STING) and Nod-like receptor protein 3. Bioinformatics analysis was carried auto to predict the association between quercetin and the SHP2/reactive oxygen species (ROS) axis. Furthermore, the effects of adenosine triphosphate (ATP) + gefitinib, SHP2 silencing and H_2O_2 on ROS levels, as well as on the p-AMP-activated protein kinase (AMPK)/XBP-1/Parkinsonism associated deglycase (DJ-1) axis, mitochondrial autophagy and apoptosis were assessed via detecting the expression levels of the corresponding proteins in cardiomyocytes by western blot analysis. JC-1 immunofluorescence was performed to evaluate mitochondrial membrane damage. The results showed that NSCLC could not significantly affect cardiac function. In addition, compared with NSCLC alone, ventricular fibrosis was exacerbated in the NSCLC + gefitinib group. However, treatment with quercetin inhibited gefitinib-induced ventricular fibrosis, activated the gefitinib-suppressed SHP2 protein expression and downregulated the gefitinib-induced XBP-1 and p-STING expression. Furthermore, the bioinformatics analysis results predicted that quercetin could interact with SHP2/ROS. The *in vitro* experiments demonstrated that the expression levels of the ROS-related proteins, namely NADPH oxidase 4 and XBP-1/DJ-1, and those of the mitochondrial autophagy- and apoptosis-related proteins were enhanced, while those of p-AMPK, were reduced in cardiomyocytes of the NSCLC + ATP + gefitinib group. However, cell treatment with quercetin inhibited ROS production and the expression levels of XBP-1/DJ-1 and apoptosis-related proteins activated by NSCLC + ATP + gefitinib. By contrast, quercetin activated the expression levels of mitochondrial autophagy-related proteins and those of p-AMPK. Furthermore, SHP2 silencing and cell treatment with H_2O_2 could separately inhibit the NSCLC + ATP + gefitinib-induced expression of mitochondrial autophagy-related proteins and p-AMPK, while they could promote ROS production and upregulate XBP-1/DJ-1 and apoptosis-related proteins. In summary, the results of the current study revealed a promising therapeutic approach for addressing cardiac issues caused by gefitinib treatment in patients with NSCLC. Therefore, quercetin could inhibit the gefitinib-induced NSCLC-mediated cardiomyocyte apoptosis via regulating the SHP2/ROS/AMPK/XBP-1/DJ-1 signaling pathway through mitochondrial autophagy.

Correspondence to: Dr Ninghua Liu, Functional Department, The Fourth Hospital of Hebei Medical University, 12 Jiankang Road, Shijiazhuang, Hebei 050000, P.R. China
E-mail: wenjian419@163.com

Key words: non-small cell lung cancer, gefitinib, pyroptosis, mitochondrial autophagy, SHP2/ROS/AMPK/XBP-1/JD-1 signaling pathway

Introduction

Epidermal growth factor receptor-tyrosine kinase inhibitors (EGFR-TKIs) are considered as one of the most significant targeted agents for the treatment of non-small cell lung cancer (NSCLC) (1). However, cardiac-related adverse events

associated with EGFR-TKI therapy can commonly occur (2) Gefitinib is an oral EGFR-TKI, which is used to treat patients with T790M-positive NSCLC, who have progressed on a standard EGFR-TKI (3). A study by Thein and Ball (4) and Soria *et al* (5) showed that gefitinib was associated with an increased risk of cardiotoxicity, prolongation of the QT interval and heart failure compared with controls. As a type of EGFR-TKI, gefitinib serves a significant role in the treatment of NSCLC. However, its potential cardiotoxicity and adverse effects need to be further investigated.

Quercetin (3,3',4',5,7-pentahydroxyflavone), a polyphenolic compound, is the most prevalent flavonoid in fruits, vegetables and medicinal plants (6). It is widely recognized that quercetin possesses antioxidant, anti-inflammatory, antimicrobial and antiparasitic activities (7-9). The anticancer effects of quercetin include its ability to promote cell viability loss, apoptosis and autophagy via regulating the phosphoinositide 3-kinase/protein kinase B/mammalian target of rapamycin, Wnt/β-catenin and mitogen-activated protein kinase (MAPK)/extracellular signal-regulated kinase 1/2 pathways (10-12). Furthermore, it has been reported that quercetin exerts protective effects against ischemic heart diseases, while it is involved in myocardial remodeling and myocardial fibrosis (13,14).

The present study was based on the concern regarding cardiac issues that could be caused by the treatment of patients with NSCLC with gefitinib. Therefore, a potential therapeutic approach for delaying gefitinib-induced cellular charring using quercetin was proposed and its underlying mechanism of action was thoroughly explored. Through *in vitro* and *in vivo* experiments, the current study aimed to reveal the role of quercetin in regulating the Src homology-2 domain-containing protein tyrosine phosphatase (SHP2)/reactive oxygen species (ROS)/AMP-activated protein kinase (AMPK)/X-box binding protein 1 (XBP-1)/Parkinsonism associated deglycase (DJ-1) signaling pathway and its inhibitory effect on gefitinib-induced cell pyroptosis in NSCLC, thus providing a significant reference and guidance for the development of more effective and safer treatment strategies for NSCLC, and further expanding the understanding of EGFR-TKI therapy-related cardiac problems in clinical practice.

Materials and methods

Animal model. Animal experiments were approved by The Fourth Hospital of Hebei Medical University Research Ethics Committee (approval no. IACUC-4th Hos Hebmu-2024022; Shijiazhuang, China). All animals were humanely cared according to the Fourth Hospital of Hebei Medical University Guide for the Care and Use of Laboratory Animals. A total of 24 mice, weighing 18.3±0.55 g, were housed in a barrier facility with a 12/12-h light/dark cycle and *ad libitum* access to food and water. A total of $5x10^6$ AC16 cells in 100 μl of PBS were injected subcutaneously into the right axilla of SPF-grade male nude mice (age, 4-5 weeks old). On the 14th day after injection, mice were randomly divided into the NSCLC, NSCLC + gefitinib and NSCLC + gefitinib + quercetin groups (n=8 mice/group). After 6 weeks, the heart tissues were collected following mice euthanasia by lethal doses of anesthetics. Animal death was verified by the lack of response to toe pinch reflex. Mice in the NSCLC + gefitinib group were injected with 40 mg/kg/day gefitinib for 14 days (2), while those in the NSCLC + gefitinib + quercetin group were intraperitoneally injected with 50 mg/kg quercetin in combination with gefitinib (15).

Ultrasonography. Doppler ultrasound was performed using the Vevo 2100 imaging system (Fujifilm VisualSonics, Inc.). Mice were first placed in an anesthesia induction chamber filled with 2.5% isoflurane in 1 l/min pure oxygen until being unresponsive to toe pinching. Subsequently, mice were placed in the supine position on a 37˚C thermostatic heating pad supplied with anesthesia airflow (1.5% isoflurane). The limbs of the mice were coated with conductive gel and affixed to electrocardiographic electrodes embedded in plates. Cardiac function was assessed via measuring left ventricular ejection fraction (LVEF) and left ventricular fold shortening (LVFS), which were calculated as the average of five consecutive cardiac cycles.

Masson's trichrome staining. Mice were euthanized by intraperitoneal injection of an overdose of sodium pentobarbital (100 mg/kg). Death was confirmed 30 min after injection by observing cardiac arrest, respiratory arrest, animal rigidity and dilated pupils. Notably, none of the mice succumbed to humane endpoints during the experimental process. Heart tissue samples were fixed in 4% paraformaldehyde, embedded in paraffin and cut into 5-μm thick sections. To assess fibrosis, Masson's trichrome staining was performed using a modified Masson's trichrome staining kit [cat. no. G1346-8 (50 ml); Beijing Solarbio Science & Technology Co., Ltd.]. Briefly, the heart tissue sections were incubated with Brinell's solution at 56˚C for 15 min and then rinsed with tap water. Subsequently, the sections were incubated with Weigert's iron hematoxylin solution followed by Biebrich scarlet-acid fuchsin solution, phospho-molybdate-phospho-tungstic acid solution and Aniline Blue solution. Finally, the slides were treated with 1% acetic acid solution, dehydrated and mounted with mounting solution.

Immunohistochemistry (IHC) staining. The expression levels of SHP2 (1:50; cat. no. ab300579), XBP-1 (20 μg/ml; cat. no. ab37152; both from Abcam), phosphorylated (p)-stimulator of interferon genes (STING; 1:200; cat. no. PA5-105674; Invitrogen; Thermo Fisher Scientific, Inc.) and Nod-like receptor protein 3 (NLRP3; 1:500; cat. no. MA5-32255; Thermo Fisher Scientific, Inc.) were detected in mouse heart tissues using IHC. More specifically, EDTA microwave heat repair was performed for 5-8 min followed by cooling at room temperature. Subsequently, the tissue sections were incubated in 3% H_2O_2 for 15 min and then with 10% goat serum (MilliporeSigma) for 30 min at 37˚C. Then, the tissue sections were incubated with a primary antibody in a wet box at 4˚C overnight, followed by incubation with the corresponding goat anti-mouse HRP-conjugated secondary antibody (1:500; cat. no. C31430100; Thermo Fisher Scientific Inc.) for 30 min at room temperature. The color was developed using the Ultra-Sensitive DAB kit (Beyotime Institute of Biotechnology). Images of the stained tissue sections were captured under a light microscope.

Bioinformatics analysis. For bioinformatics analysis the 'geoquery' (version 2.64.2; bioconductor.org/packages/release/bioc/html/geoquery.html), 'limma' (version 3.52.2; bioconductor.org/packages/release/bioc/html/limma.html), 'ggplot2' (version 3.3.6; ggplot2.tidyverse.org/) and 'ComplexHeatmap' (version 2.13.1; jokergoo.github.io/ComplexHeatmap/) software in 'R' (version 4.2.1; www.R-project.org/) package were utilized. The GSE18842 dataset was downloaded from the Gene Expression Omnibus (GEO) database via the 'GEOquery' package. The missing values were completed using the 'impute' package (16). The data were normalized using the 'normalizeBetweenArrays' function in 'limma' package and box plots were constructed with the 'ggplot2' package. For the differential analysis a threshold of |LogFC|>1 and P<0.05 was set and the results were and visualized using the 'ggplot2' package. The rows were normalized and clustered to Euclidean distance. The columns were not clustered. The heatmaps of the differentially expressed genes were constructed using the 'ComplexHeatmap' package. The target genes of quercetin were retrieved from the DrugBank database (https://go.drugbank.com/). A total of 29 target genes were identified and were then analyzed for shared genes with NSCLC. The results were visualized using the 'ggplot2' (version 3.3.6) and 'VennDiagram' (version 1.7.3; cran.r-project.org/web/packages/VennDiagram/index.html) packages. In addition, proteins with a confidence level of ≥0.9 were selected in STRING database (https://string-db.org). The proteins in the input list were analyzed for protein-protein interactions (PPI) and the hub genes, which were enriched using 'R' (version 4.2.1) package, were visualized using the Cytoscape software (https://cytoscape.org/). Additionally, the 'clusterProfiler' (version 4.4.4; https://bioconductor.org/packages/release/bioc/html/clusterProfiler.html), 'GOplot' (version 1.0.2; github.com/GuangchuangYu/GOplot), 'ggplot2' (version 3.3.6) in 'R' (version 4.2.1) package and the 'ID conversion' and 'org.Hs.eg.db' packages were used. The 'Species' option was set to 'Human (Homo sapiens)'. P<0.05 was considered to indicate differentially expressed genes. Gene clusters and pathways with biometric differences between Hub genes were screened out and the enrichment analysis results were visualized using the 'ggplot2' package.

Cell culture and grouping. AC16 cardiomyocytes were purchased from the Cell Bank of the Chinese Academy of Sciences. Cells were co-cultured in Coning chambers. When needed, cells were treated with gefitinib (0.1 μmol/l, cat. no. MB1112; Dalian Meilun Biology Technology Co., Ltd.) and incubated at 37˚C in an incubator with 5% CO_2. For cell transfection, cardiomyocytes were cultured in serum-free medium at 37˚C and 5% CO_2. When reached 80% confluency, cells were transfected with the indicated short hairpin (sh) RNAs or scrambled shRNA (Thermo Fisher Scientific, Inc.) for 48 h. The plasmid (2.0 μg) was transfected with Lipofectamine 2000 (Invitrogen; Thermo Fisher Scientific, Inc.) according to the manufacturer's protocol. Cells were incubated at 37˚C (5% CO_2) for 12 h and the medium was replaced with growth medium containing FBS. Incubation was continued for 48 h after transfection. The shRNA sequence used for SHP2 was 5'-GAAGCACAGUACCGAUUUA-3'. All cell lines were cultured in DMEM and were treated with 4.3 mM ATP, 100 nM gefitinib (17), 80 μM quercetin and 200 μM H_2O_2 for 48 h.

Shp-2 knockdown efficiency. RNA was harvested from tumour cells collected from mice using TRIzol reagent (Ambion; Thermo Fisher Scientific, Inc.) and cDNA was obtained using HiScript III RT SuperMix (Vazyme Biotech Co., Ltd.) catalyzed by using mRNA as template. The mRNA primer sequences were used as shown in Table SI. chamQ SYBR qPCR Master Mix (Vazyme Biotech Co., Ltd.) was used for fluorescence quantification. GAPDH was used as an internal control, and the relative gene expression was normalized using the $2^{-\Delta\Delta Cq}$ method (18). Transfection efficiency, verified using PCR, is demonstrated in Fig. S1.

Western blot analysis. Heart tissues or cells were homogenized and lysed in RIPA buffer (154 mM NaCl, 0.25% sodium deoxycholate, 1% NP-40, 0.8 mM EDTA and 65.2 mM Tris base) supplemented with a mixture of protease inhibitors. Then, 20 μg of total proteins were separated by 10% SDS-PAGE (Invitrogen; Thermo Fisher Scientific, Inc.) and were then transferred onto a PVDF membrane. The membrane was blocked with 0.1% TBS-Tween-20 (TBST) containing 5% skimmed milk for 1 h. The primary antibodies used were as follows: Anti-NADPH oxidase 4 (NOX4; 1:1,000; cat. no. ab112414), anti-SHP2 (1:1,000; cat. no. ab300579), anti-p-AMPK (1:1,000; cat. no. 133448), anti-XBP-1 (1:1,000; cat. no. ab31752), anti-DJ-1 (1:1,000; cat. no. ab76008), anti-PTEN-induced putative kinase (PINK; 1:1,000; cat. no. 216144), anti-beclin1 (1:1,000; cat. no. ab302669), anti-p-STING (1:1,000; cat. no. ab2239074), p-interferon regulatory factor 3 (IRF3; 1:1,000; cat. no. ab76493), NLRP3 (1:1,000; cat. no. ab263899), anti-gasdermin D (GSDMD; 1:1,000; cat. no. 219800), IL-β (1:1,000; cat. no. ab283818), peroxisome proliferator-activated receptor-γ (PPAR-γ; 1:1,000; cat. no. ab178860), PGC-1 (1:1,000; cat. no. ab310323) and anti-GAPDH (1:1,000; cat. no. ab8245; all from Abcam). The membrane was incubated with the corresponding HRP-conjugated secondary antibodies (Goat Anti-Rabbit IgG H&L; 1:5,000; cat. no. ab205718; Abcam) at room temperature for 1 h, followed by washing with TBST for three times. The protein bands were visualized using an ECL kit (Thermo Fisher Scientific, Inc.). Quantification was performed using the Quantity One system (Bio-Rad Laboratories, Inc.). GAPDH served as an internal control.

5,5',6,6'-tetrachloro-1,1',3,3'-tetraethylbenzimidazol-carbocyanine iodide (JC-1) assay. Equal amounts of cardiomyocytes ($5x10^5$ cells/ml) were inoculated onto 8-well culture slides (BD Falcon™; BD Biosciences) and 24 h later were processed as previously described (19). Following washing with PBS, cells were incubated in fresh medium supplemented with JC-1 for 15 min. The cells were then washed with PBS to remove the staining solution and were supplemented with fresh medium. Subsequently, cells were immediately observed under a fluorescence microscope.

Statistical analysis. All data are expressed as the mean ± SEM of at least three independent experiments. The differences between two groups were compared using Student's t-test

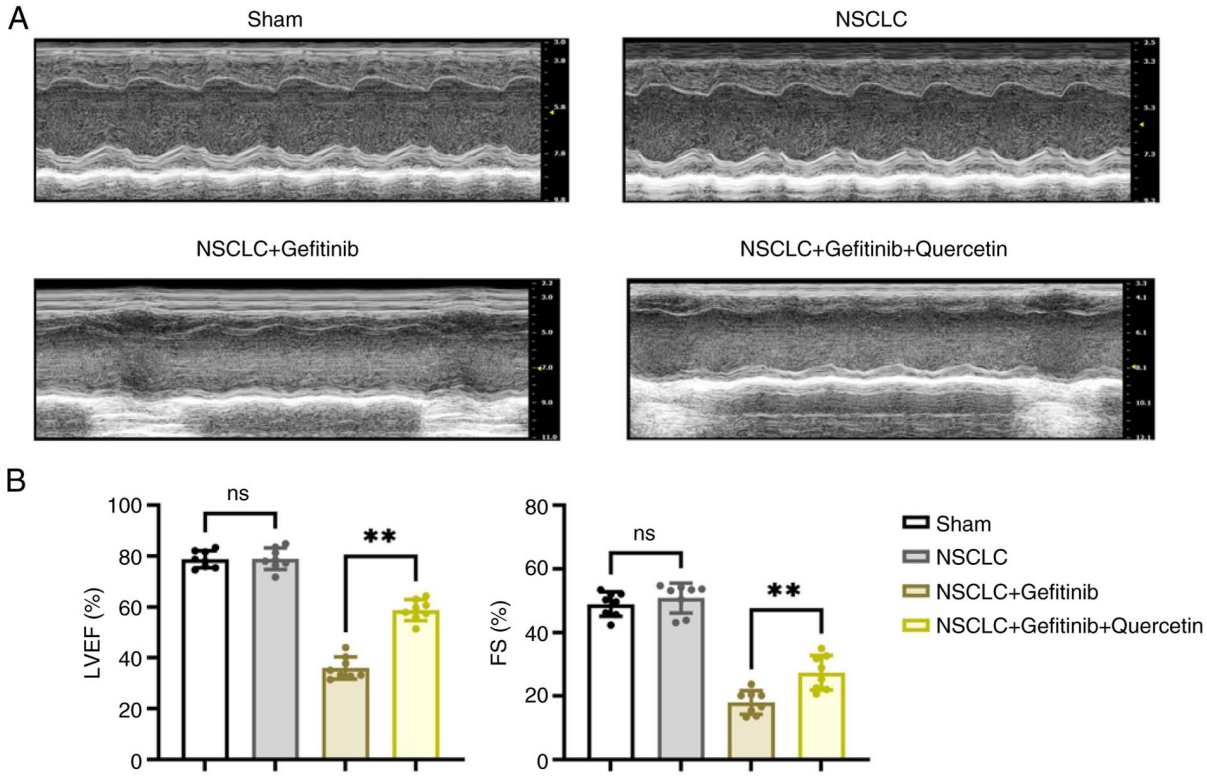

Figure 1. Quercetin improves cardiac function in gefitinib-treated mice with NSCLC. (A) Representative echocardiography images from each group are shown. (B) Cardiac function was assessed by quantitatively analyzing LVEF and FS (n=8). **P<0.01. NSCLC, non-small cell lung cancer; LVEF, left ventricular ejection fraction; FS, fractional shortening; ns, not significant (P>0.05).

(paired t-test). Comparisons between multiple groups were performed by one-way analysis of variance followed by Tukey/Bonferroni post hoc test. All statistical analyses were performed using GraphPad Prism 5.0 software (GraphPad Software, Inc.; Dotmatics). P<0.05 was considered to indicate a statistically significant difference.

Results

Quercetin improves cardiac function in gefitinib-treated NSCLC mice. Firstly, the present study aimed to uncover the role of quercetin in improving cardiac function in gefitinib-treated NSCLC mice. The ultrasonic inspection results are shown in Fig. 1. Treatment of NSCLC mice with gefitinib significantly attenuated cardiac function, as evidenced by the reduced FS and LVEF (~50%). This finding indicated that cardiac contraction and relaxation were significantly impaired. However, mice co-treatment with quercetin significantly improved cardiac function via increasing FS and LVEF by ~30%.

Quercetin ameliorates cardiac fibrosis in gefitinib-treated mice with NSCLC via the SHP2/XBP-1/p-STING signaling pathway. To detect changes in collagen content, fibrogenesis was assessed by Masson's trichrome staining. The results revealed that NSCLC had no significant effect on cardiomyocyte function. However, treatment with gefitinib exacerbated ventricular fibrosis compared with the NSCLC group, as evidenced by the large and intense accumulation of collagen. Furthermore, co-treatment with quercetin inhibited the gefitinib-induced ventricular fibrosis (Fig. 2A). In addition, IHC staining of mouse heart tissues revealed that the protein expression levels of SHP2 were reduced, while those of XBP-1, p-STING and NLRP3 were increased in the NSCLC + gefitinib group compared with the NSCLC group. However, mice treatment with quercetin abrogated the effects of gefitinib on the expression levels of the aforementioned proteins (Fig. 2B).

Quercetin is associated with 'SHP2/ROS signaling', 'chemical carcinogenesis-receptor' and 'antigen processing and presentation'. The 91 sets of samples obtained in the GSE18842 dataset were divided into two groups, namely the control and cancer groups. A total of 2,545 differentially expressed molecules were identified, including 1,119 upregulated and 1,426 downregulated ones. The differentially expressed genes are visualized in a volcano plot (Fig. 3A). The top 20 upregulated and downregulated genes were also visualized in the form of a heat map (Fig. 3B). The 13 common genes between quercetin and NSCLC were visualized by a Wayne diagram (Fig. 3C). Additionally, the STRING online database was used to construct a PPI network of the 11 target proteins (Fig. 3D). The interaction network between the drug and the eight hub genes was constructed using 'Cytoscape' (version 3.9.1) (Fig. 3E). Gene Ontology (GO) and Kyoto Encyclopedia of Genes and Genomes (KEGG) enrichment analyses were performed to create a biological process network of the differentially expressed genes. These analyses are used to classify the results of functional annotation into the following three categories: Biological process, cellular component and molecular function. GO (Fig. 3F) and KEGG

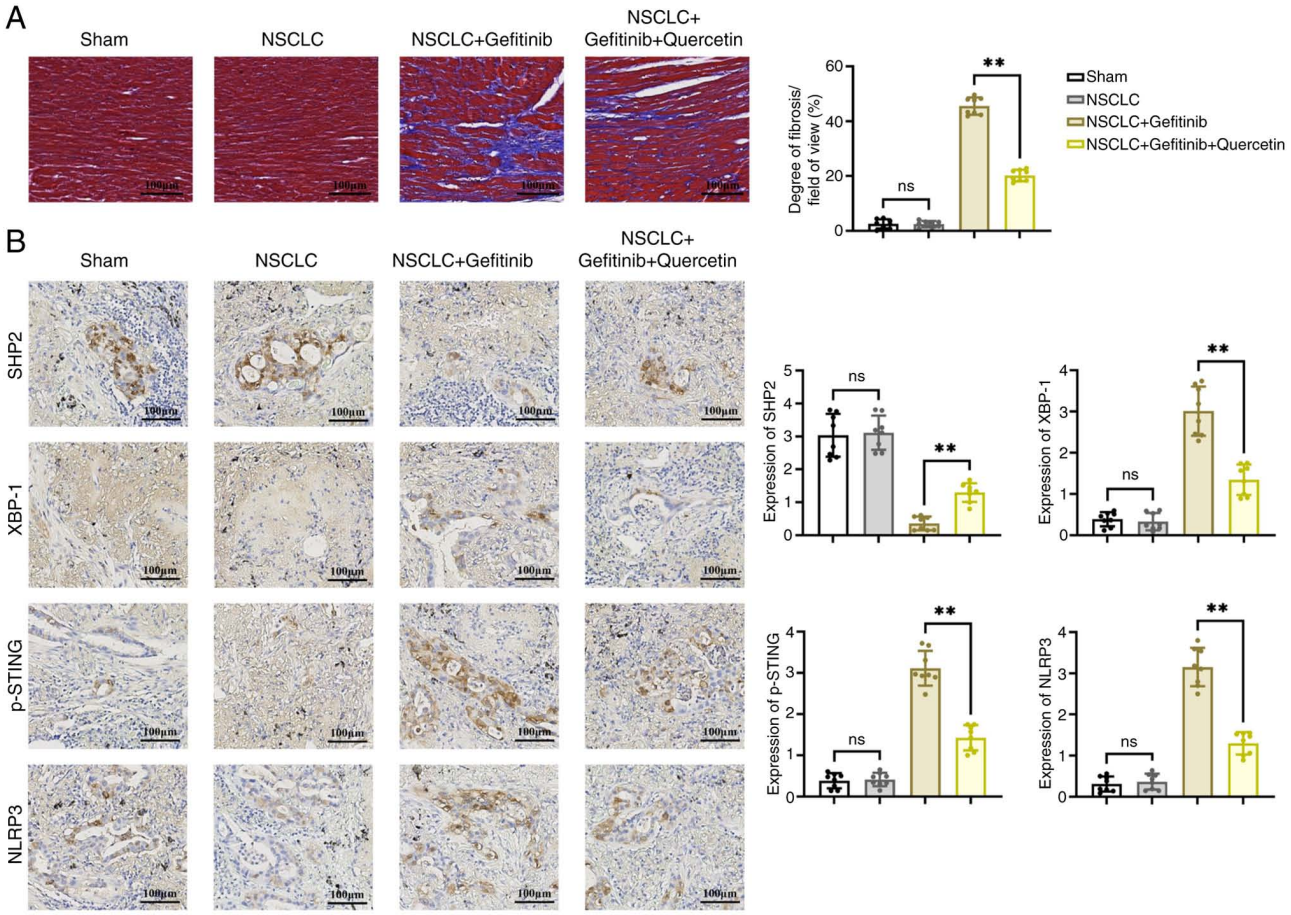

Figure 2. Quercetin ameliorates cardiac fibrosis in gefitinib-treated mice with NSCLC through the SHP2/XBP-1/p-STING signaling pathway. Mouse heart (A) Masson's trichrome and (B) immunohistochemistry staining results are presented. **P<0.01. NSCLC, non-small cell lung cancer; SHP2, Src homology-2 domain-containing protein tyrosine phosphatase; XBP-1, X-box binding protein 1; p-STING, phosphorylated stimulator of interferon genes; NLRP3, Nod-like receptor protein; ns, not significant (P>0.05).

(Fig. 3G) analyses revealed that quercetin was mainly enriched in the terms 'SHP2/ROS signaling pathway', 'chemical carcinogenesis-receptor' and 'antigen processing and presentation'.

Quercetin regulates myocardial cell mitochondrial autophagy via the ROS/SHP2 and p-AMPK/XBP-1S/DJ-1 pathways. To further explore whether quercetin could regulate mitochondrial autophagy the ROS/SHP2 axis, cardiomyocytes were transfected with shSHP2 or stimulated with H_2O_2. The western blot results from the *in vitro* experiments revealed that the expression levels of the ROS-related proteins, NOX4, XBP-1 and DJ-1, and those of the mitochondrial autophagy-related proteins, PINK, parkin and beclin1, were increased, while those of p-AMPK were reduced in cardiomyocytes in the NSCLC + gefitinib group. Treatment with quercetin abrogated the aforementioned effects. However, SHP2 silencing or cell treatment with H_2O_2 suppressed the protein expression levels of PINK, parkin, beclin1 and p-AMPK, and promoted the expression levels of NOX4, XBP-1 and DJ-1 proteins (Fig. 4A and B).

Quercetin regulates myocardial cell mitochondrial function and the expression of apoptosis-related proteins via ROS/SHP2. Mitochondrial membrane potential (MMP) was assessed using JC-1 staining. The results demonstrated that MMP was significantly reduced in the NSCLC + gefitinib group, as evidenced by the enhanced blue/red fluorescence ratio. Additionally, western blot analysis demonstrated that the expression levels of PPAR-γ and PGC-1 were reduced, while those of the cellular scorch death-related proteins, p-STING/p-IRF3/NLRP3/GSDMD/IL-1, were significantly increased in the NSCLC + gefitinib group. However, MMP was enhanced after quercetin treatment, accompanied by PPAR-γ/PGC-1 upregulation and p-STING/p-IRF3/NLRP3/GSDMD/IL-1β downregulation. Furthermore, cell transfection with shSHP2 or treatment with H_2O_2 significantly reduced MMP, downregulated PPAR-γ and PGC-1, and upregulated p-STING, p-IRF3, NLRP3, GSDMD and IL-1β (Fig. 5).

Discussion

Lung cancer is the most common type of cancer worldwide. By the time it is diagnosed, it has usually spread. As a result, surgery is not commonly applicable and, therefore, medication, usually chemotherapy, is needed. NSCLC is the most frequent type of lung cancer, which is more commonly treated with TKIs (20). More specifically, TKIs are considered as the standard treatment approach for EGFR-mutated NSCLC with brain metastases. A recent study revealed that EGFR-TKIs

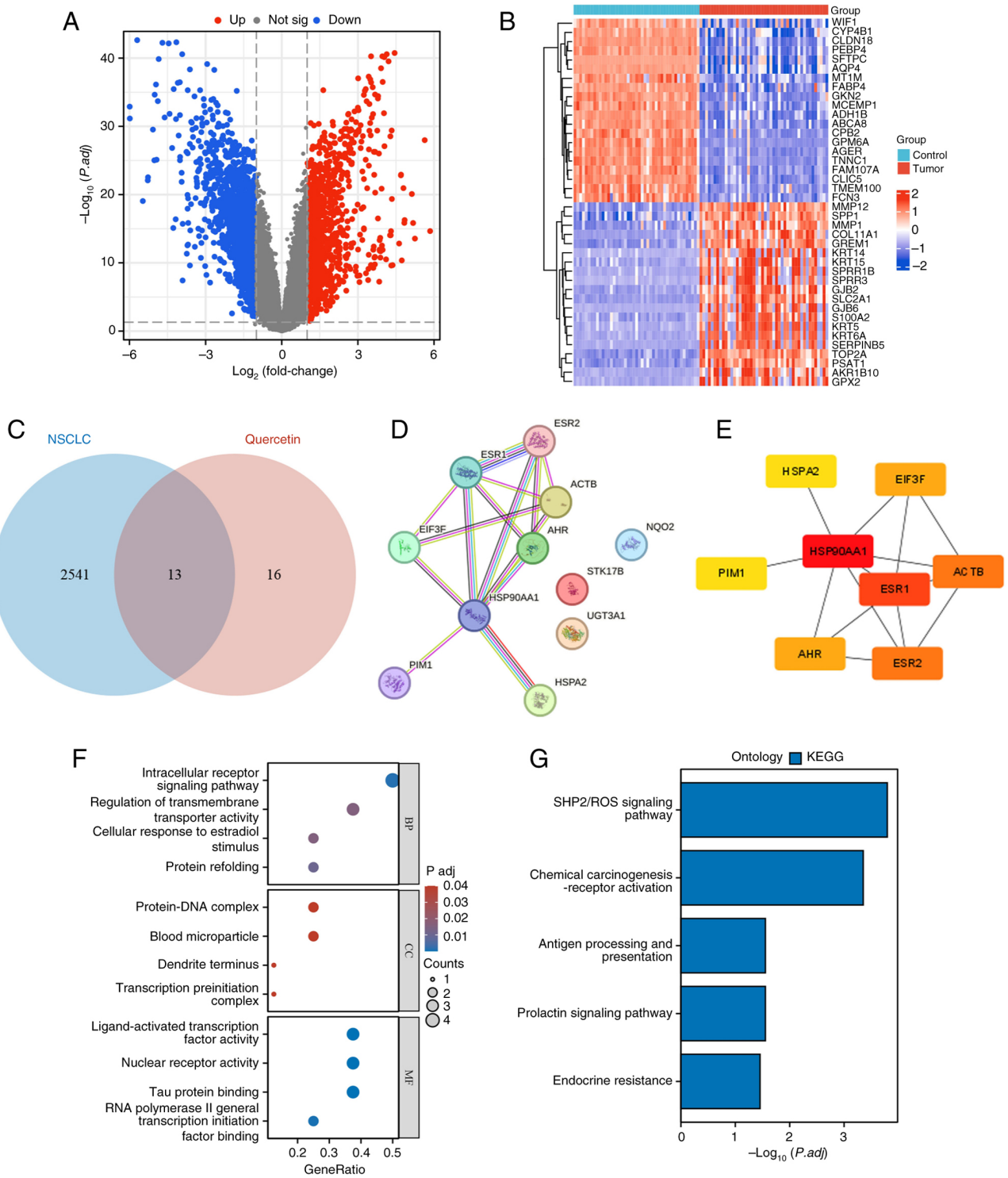

Figure 3. Quercetin regulates myocardial cell mitochondrial autophagy via the ROS/SHP2 and phosphorylated-AMP-activated protein kinase/X-box binding protein 1/DJ-1 pathway. (A) The results of variance analysis are illustrated as Volcano plots. (B) The top 20 upregulated and downregulated genes are shown in a heat map. (C) Wayne's plot of the 13 shared genes between quercetin and NSCLC. (D) The protein-protein interaction analysis network map of the 11 target proteins is shown. (E) Interaction network mapping. (F) Gene Ontology analysis. (G) KEGG analysis. ROS, reactive oxygen species; SHP2, Src homology-2 domain-containing protein tyrosine phosphatase; NSCLC, non-small cell lung cancer; KEGG, Kyoto Encyclopedia of Genes and Genomes; BP, biological process; CC, cellular component; MF, molecular function.

combined with chemotherapy could improve progression-free survival in patients with EGFR-mutated advanced NSCLC (21).

It has been reported that the mechanism of action of gefitinib in lung cancer is extremely complex and diverse. Firstly, it can activate the inositol-requiring enzyme 1α/XBP-1 signaling pathway via releasing intracellular Ca^{2+} and entering the endoplasmic reticulum through the ATP/P2X7 purinergic receptor pathway (22,23). This process not only inhibits the mitochondrial autophagy process, but also further activates the DJ-1/transcription factor EB signaling

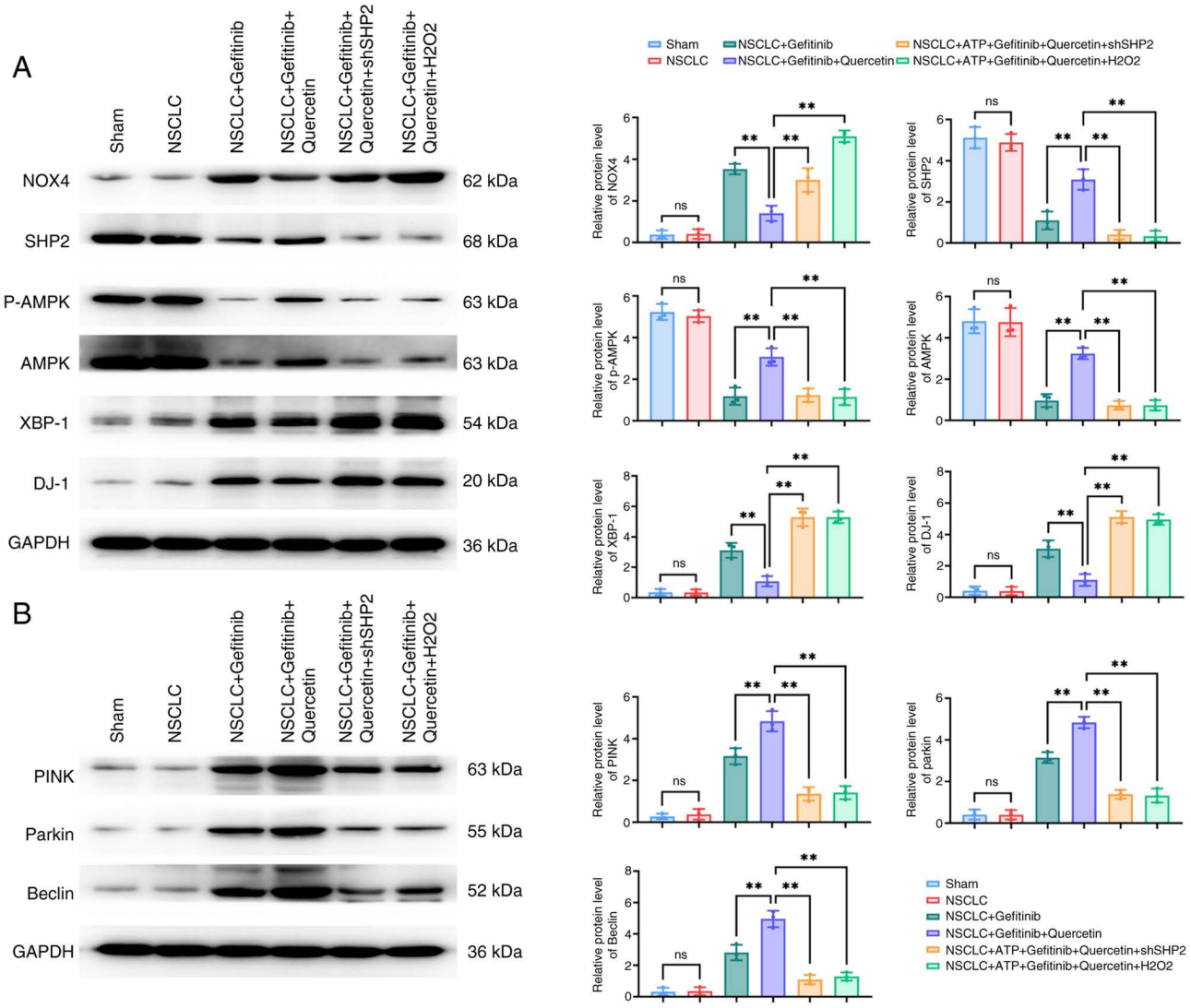

Figure 4. Quercetin regulates p-AMPK/XBP-1/DJ-1-mediated mitochondrial autophagy in cardiomyocytes via ROS/SHP2. (A and B) The expression levels of (A) the p-AMPK/XBP-1S/DJ-1 axis-related and (B) mitochondrial autophagy-related, PTEN-induced putative kinase/parkin/beclin1, proteins in ROS/SHP2-regulated cardiomyocytes treated with quercetin were detected by western blot analysis. **P<0.01. p-AMPK, phosphorylated AMP-activated protein kinase; XBP-1, X-box binding protein 1; ROS, reactive oxygen species; SHP2, Src homology-2 domain-containing protein tyrosine phosphatase; NOX4, NADPH oxidase 4; sh-, short hairpin; NSCLC, non-small cell lung cancer; ns, not significant (P>0.05).

pathway (24,25), which is in turn involved in maintaining the normal metabolic function and homeostasis in cells. In addition, gefitinib was also experimentally found to act via activating the ROS signaling pathway. ROS is possibly involved in this process through the SHP2-induced inhibition of the MAPK signaling pathway (26), thus further blocking mitochondrial autophagy (27,28). Other studies also indicated that mitochondrial autophagy could maintain cell survival and function via inhibiting the mtDNA/cGAS signaling pathway-induced activation of the STING/IRF3/NLRP3/GSDMD/IL-1β signaling pathway, thus attenuating cell pyroptosis (29,30).

Numerous *in vitro* and *in vivo* studies have suggested that quercetin exerts a variety of functions, such as anti-inflammatory, antioxidant, antihypertensive, hypoglycemic, neurovascular protective, anticancer, anti-aging and immune-enhancing properties (31). Quercetin, as a natural compound, has also attracted marked attention in the field of anticancer therapy. Emerging evidence has suggested that quercetin exerts a particular inhibitory effect on several types of cancer, including lung cancer. Therefore, a previous study revealed that quercetin inhibited tumor cell proliferation, invasion and metastasis, while inducing cell apoptosis (32). In addition, quercetin could also display anticancer effects via regulating the tumor microenvironment and affecting tumor angiogenesis (33,34). Quercetin has also attracted increasing attention in NSCLC. Therefore, previous experimental studies showed that quercetin treatment enhanced the efficacy of chemotherapy or targeted therapy, reduced tumor resistance to chemotherapeutic drugs and prolong patient survival. In addition, it has been reported that quercetin can also play an anti-lung cancer role via regulating the activation of lung cancer-related signaling pathways, cell proliferation, apoptosis and metastasis.

In the present study, the effects of quercetin on gefitinib-induced heart problems in patients with NSCLC and its mechanism of action were investigated. Therefore, the experimental results

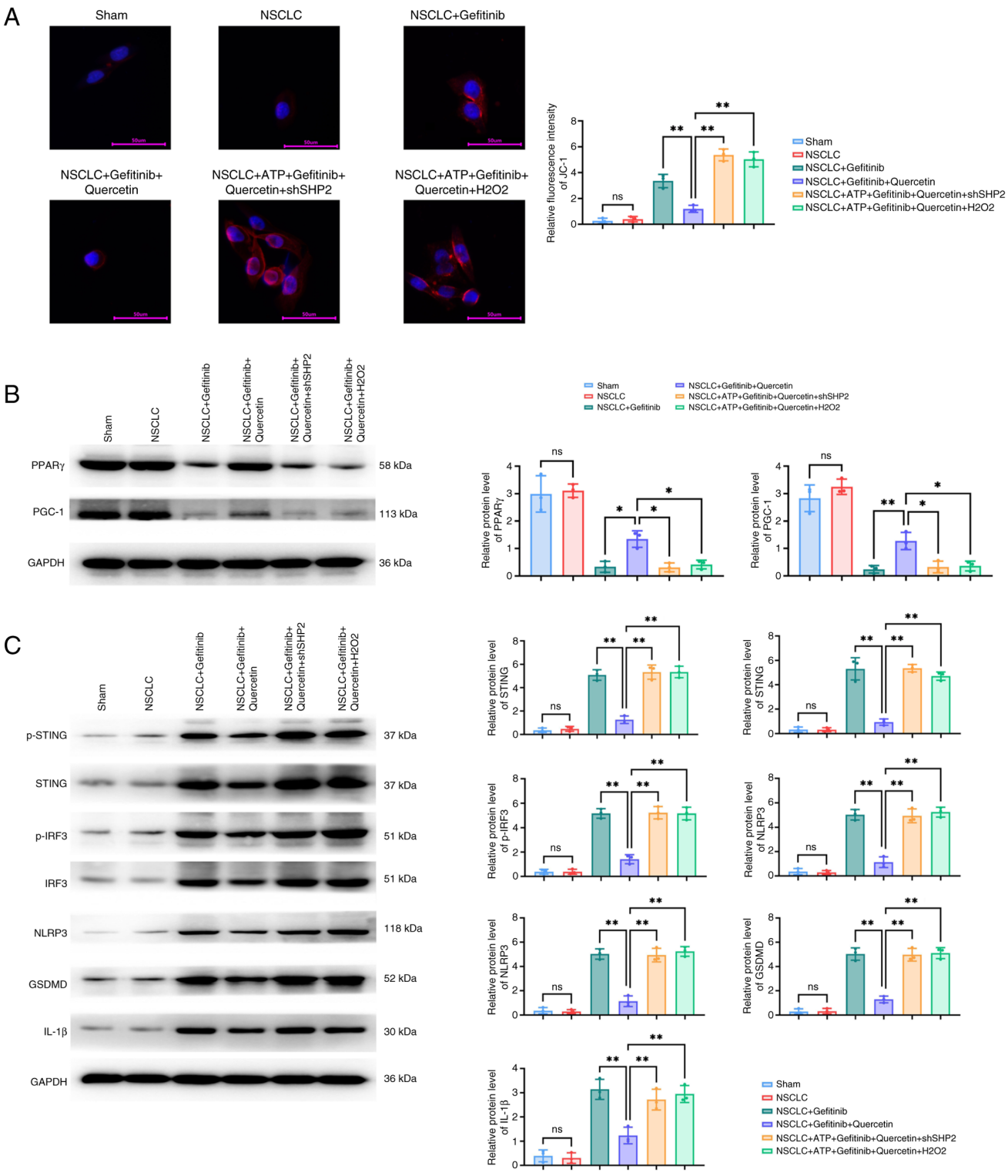

Figure 5. Protein expression levels of the p-STING/p-IRF3/NLRP3/GSDMD/IL-1β pathway-related proteins in quercetin-treated and ROS/SHP2-regulated cardiomyocytes. (A) Immunofluorescence staining of JC-1 in cardiomyocytes treated with quercetin. The protein expression levels of the (B) mitochondrial autophagy-related proteins, PPAR-γ and PPAR-γ coactivator-1, and (C) those of the p-STING/p-IRF3/NLRP3/GSDMD/IL-1β pathway were detected in quercetin-treated ROS/SHP2-regulated cardiomyocytes by western blot analysis. *P<0.05 and **P<0.01. p-STING, phosphorylated stimulator of interferon genes; IRF3, interferon regulatory factor 3; NLRP3, Nod-like receptor protein 3; GSDMD, gasdermin D; ROS, reactive oxygen species; SHP2, Src homology-2 domain-containing protein tyrosine phosphatase; PPAR-γ, peroxisome proliferator-activated receptor γ; PGC-1, PPAR-γ coactivator; NSCLC, non-small cell lung cancer; ns, not significant (P>0.05).

identified that gefitinib could promote cardiac fibrosis and cellular focal death, while the application of quercetin could effectively suppress the occurrence of these adverse effects. More specifically, quercetin could attenuate gefitinib-induced cell pyroptosis via modulating mitochondrial autophagy mediated by the SHP2/ROS/AMPK/XBP-1/DJ-1 signaling pathway.

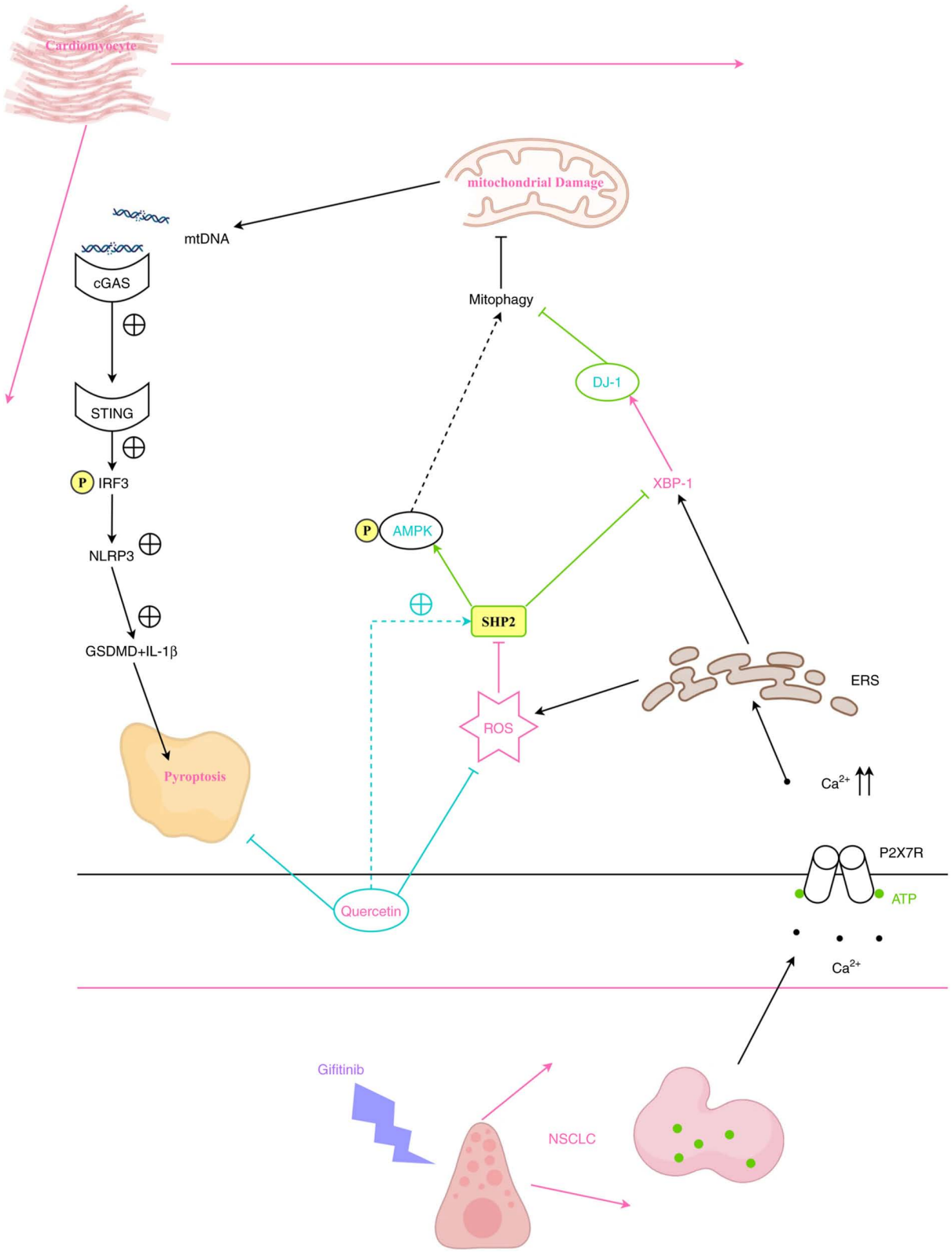

Figure 6. Quercetin inhibits gefitinib-activated cell death in NSCLC via regulating SHP2/ROS/AMPK/XBP-1/DJ-1 signaling pathway-mediated mitochondrial autophagy. NSCLC, non-small cell lung cancer; SHP2, Src homology-2 domain-containing protein tyrosine phosphatase; ROS, reactive oxygen species; AMPK, AMP-activated protein kinase; GSDMD, gasdermin D; STING, stimulator of interferon genes; cGAS, cyclic GMP-AMP synthase; IRF3, interferon regulatory factor 3; mtDNA, mitochondrial DNA; ERS, endoplasmic reticulum stress.

The bioinformatics analysis results verified the association between quercetin and SHP2/ROS signaling, thus further supporting the effect of quercetin on regulating heart disorders. The results of the *in vitro* experiments revealed that quercetin treatment abrogated the effects of gefitinib on ROS production and the expression of related proteins, accompanied by the enhanced expression of mitochondrial autophagy-related proteins and p-AMPK, thus maintaining

the stability of cardiac function. In addition, the results showed that quercetin could protect mitochondrial integrity and attenuate the decrease in MPP, as evidenced by the assessment of mitochondrial membrane damage via JC-1 staining. This finding provided additional evidence for the effect of quercetin on preventing cellular focal death.

Taken together, the results of the present study indicated that quercetin could be considered as a potential therapeutic approach to effectively delay cardiac issues in patients with NSCLC treated with gefitinib. Quercetin could inhibit cell pyroptosis via modulating mitochondrial autophagy mediated by the SHP2/ROS/AMPK/XBP-1/DJ-1 signaling pathway, thus providing a significant reference and novel insights into the development of more effective and safer therapeutic strategies for NSCLC. The current study could also provide substantial guidance and insights for exploring the mechanisms underlying the effect of EGFR-TKIs on promoting the onset of cardiac issues in clinical practice (Fig. 6).

Acknowledgements

Not applicable.

Funding

No funding was received.

Availability of data and materials

The data generated in the present study may be requested from the corresponding author.

Authors' contributions

JZ conceived and designed the experiments. JZ, SQ, YD, HD and NL performed the experiments. JZ, SQ and HD analysed the data. JZ wrote the manuscript. JZ, SQ, YD, HD and NL confirm the authenticity of all the raw data. All authors read and approved the final version of the manuscript.

Ethics approval and consent to participate

The study protocol was approved (approval no. IACUC-4th Hos Hebmu-2024022) by The Fourth Hospital of Hebei Medical University Research Ethics Committee (Shijiazhuang, China).

Patient consent for publication

Not applicable.

Competing interests

The authors declare that they have no competing interests.

References

1. Pan Z, Wang K, Wang X, Jia Z, Yang Y, Duan Y, Huang L, Wu ZX, Zhang JY and Ding X: Cholesterol promotes EGFR-TKIs resistance in NSCLC by inducing EGFR/Src/Erk/SP1 signaling-mediated ERRα re-expression. Mol Cancer 21: 77, 2022.
2. Cheng C, Wang S, Dong J, Zhang S, Yu D and Wang Z: Effects of targeted lung cancer drugs on cardiomyocytes studied by atomic force microscopy. Anal Methods 15: 4077-4084, 2023.
3. Mok TS, Wu YL, Ahn MJ, Garassino MC, Kim HR, Ramalingam SS, Shepherd FA, He Y, Akamatsu H, Theelen WS, *et al*: Osimertinib or platinum-pemetrexed in EGFR T790M-positive lung cancer. N Engl J Med 376: 629-640, 2017.
4. Thein KZ, Swarup S, Ball S, Quirch M, Vorakunthada Y, Htwe KK, D'Cunha N, Hardwicke F, Awasthi S and Tijani L: 1388P Incidence of cardiac toxicities in patients with advanced non-small cell lung cancer treated with osimertinib: A combined analysis of two phase III randomized controlled trials. Ann Oncol 29: viii500, 2018.
5. Soria JC, Ohe Y, Vansteenkiste J, Reungwetwattana T, Chewaskulyong B, Lee KH, Dechaphunkul A, Imamura F, Nogami N, Kurata T, *et al*: Osimertinib in untreated EGFR-mutated advanced non-small-cell lung cancer. N Engl J Med 378: 113-125, 2018.
6. Wang M, Chen X, Yu F, Zhang L, Zhang Y and Chang W: The targeting of noncoding RNAs by quercetin in cancer prevention and therapy. Oxid Med Cell Longev 2022: 4330681, 2022.
7. Güran M, Şanlıtürk G, Kerküklü NR, Altundağ EM and Süha Yalçın A: Combined effects of quercetin and curcumin on anti-inflammatory and antimicrobial parameters in vitro. Eur J Pharmacol 859: 172486, 2019.
8. Ersoz M, Erdemir A, Derman S, Arasoglu T and Mansuroglu B: Quercetin-loaded nanoparticles enhance cytotoxicity and antioxidant activity on C6 glioma cells. Pharm Dev Technol 25: 757-766, 2020.
9. Sul OJ and Ra SW: Quercetin Prevents LPS-induced oxidative stress and inflammation by modulating NOX2/ROS/NF-kB in lung epithelial cells. Molecules 26: 6949, 2021.
10. Lan CY, Chen SY, Kuo CW, Lu CC and Yen GC: Quercetin facilitates cell death and chemosensitivity through RAGE/PI3K/AKT/mTOR axis in human pancreatic cancer cells. J Food Drug Anal 27: 887-896, 2019.
11. Hasan AAS, Kalinina EV, Tatarskiy VV, Volodina YL, Petrova AS, Novichkova MD, Zhdanov DD and Shtil AA: Suppression of the antioxidant system and PI3K/Akt/mTOR signaling pathway in cisplatin-resistant cancer cells by quercetin. Bull Exp Biol Med 173: 760-764, 2022.
12. Li X, Zhou N, Wang J, Liu Z, Wang X, Zhang Q, Liu Q, Gao L and Wang R: Quercetin suppresses breast cancer stem cells (CD44(+)/CD24(-)) by inhibiting the PI3K/Akt/mTOR-signaling pathway. Life Sci 196: 56-62, 2018.
13. Zhou Y, Suo W, Zhang X, Lv J, Liu Z and Liu R: Roles and mechanisms of quercetin on cardiac arrhythmia: A review. Biomed Pharmacother 153: 113447, 2022.
14. Wang L, Tan A, An X, Xia Y and Xie Y: Quercetin dihydrate inhibition of cardiac fibrosis induced by angiotensin II in vivo and in vitro. Biomed Pharmacother 127: 110205, 2020.
15. Huang KY, Wang TH, Chen CC, Leu YL, Li HJ, Jhong CL and Chen CY: Growth suppression in lung cancer cells harboring EGFR-C797S mutation by quercetin. Biomolecules 11: 1271, 2021.
16. Barretina J, Caponigro G, Stransky N, Venkatesan K, Margolin AA, Kim S, Wilson CJ, Lehár J, Kryukov GV, Sonkin D, *et al*: The cancer cell line encyclopedia enables predictive modelling of anticancer drug sensitivity. Nature 483: 603-607, 2012.
17. Heliste J, Jokilammi A, Vaparanta K, Paatero I and Elenius K: Combined genetic and chemical screens indicate protective potential for EGFR inhibition to cardiomyocytes under hypoxia. Sci Rep 11: 16661, 2021.
18. Livak KJ and Schmittgen TD: Analysis of relative gene expression data using real-time quantitative PCR and the 2(-Delta Delta C(T)) method. Methods 25: 402-408, 2001.
19. Sunasee R, Araoye E, Pyram D, Hemraz UD, Boluk Y and Ckless K: Cellulose nanocrystal cationic derivative induces NLRP3 inflammasome-dependent IL-1β secretion associated with mitochondrial ROS production. Biochem Biophys Rep 4: 1-9, 2015.
20. Greenhalgh J, Boland A, Bates V, Vecchio F, Dundar Y, Chaplin M and Green JA: First-line treatment of advanced epidermal growth factor receptor (EGFR) mutation positive non-squamous non-small cell lung cancer. Cochrane Database Syst Rev 3: CD010383, 2021.

21. Hou X, Li M, Wu G, Feng W, Su J, Jiang H, Jiang G, Chen J, Zhang B, You Z, *et al*: Gefitinib plus chemotherapy vs gefitinib alone in untreated EGFR-mutant non-small cell lung cancer in patients with brain metastases: The GAP BRAIN open-label, randomized, multicenter, phase 3 study. JAMA Netw Open 6: e2255050, 2023.
22. Wilkaniec A, Cieślik M, Murawska E, Babiec L, Gąssowska-Dobrowolska M, Pałasz E, Jęśko H and Adamczyk A: P2X7 receptor is involved in mitochondrial dysfunction induced by extracellular alpha synuclein in neuroblastoma SH-SY5Y cells. Int J Mol Sci 21: 3959, 2020.
23. Hong Y, Zhou X, Li Q, Chen J, Wei Y, Long C, Shen L, Zheng X, Li D, Wang X, *et al*: X-box binding protein 1 caused an imbalance in pyroptosis and mitophagy in immature rats with di-(2-ethylhexyl) phthalate-induced testis toxicity. Genes Dis 11: 935-951, 2024.
24. Imberechts D, Kinnart I, Wauters F, Terbeek J, Manders L, Wierda K, Eggermont K, Madeiro RF, Sue C, Verfaillie C and Vandenberghe W: DJ-1 is an essential downstream mediator in PINK1/parkin-dependent mitophagy. Brain 145: 4368-4384, 2022.
25. Xu M, Hang H, Huang M, Li J, Xu D, Jiao J, Wang F, Wu H, Sun X, Gu J, *et al*: DJ-1 deficiency in hepatocytes improves liver ischemia-reperfusion injury by enhancing mitophagy. Cell Mol Gastroenterol Hepatol 12: 567-584, 2021.
26. Zhu G, Xie J, Kong W, Xie J, Li Y, Du L, Zheng Q, Sun L, Guan M, Li H, *et al*: Phase separation of disease-associated SHP2 mutants underlies MAPK hyperactivation. Cell 183: 490-502.e18, 2020.
27. Li Y, Chen H, Xie X, Yang B, Wang X, Zhang J, Qiao T, Guan J, Qiu Y, Huang YX, *et al*: PINK1-mediated mitophagy promotes oxidative phosphorylation and redox homeostasis to induce drug-tolerant persister cancer cells. Cancer Res 83: 398-413, 2023.
28. Liu H, Ho PW, Leung CT, Pang SY, Chang EES, Choi ZY, Kung MH, Ramsden DB and Ho SL: Aberrant mitochondrial morphology and function associated with impaired mitophagy and DNM1L-MAPK/ERK signaling are found in aged mutant Parkinsonian LRRK2^{R1441G} mice. Autophagy 17: 3196-3220, 2021.
29. Luo T, Jia X, Feng WD, Wang JY, Xie F, Kong LD, Wang XJ, Lian R, Liu X, Chu YJ, *et al*: Bergapten inhibits NLRP3 inflammasome activation and pyroptosis via promoting mitophagy. Acta Pharmacol Sin 44: 1867-1878, 2023.
30. Liu Z, Wang M, Wang X, Bu Q, Wang Q, Su W, Li L, Zhou H and Lu L: XBP1 deficiency promotes hepatocyte pyroptosis by impairing mitophagy to activate mtDNA-cGAS-STING signaling in macrophages during acute liver injury. Redox Biol 52: 102305, 2022.
31. Di Petrillo A, Orrù G, Fais A and Fantini MC: Quercetin and its derivates as antiviral potentials: A comprehensive review. Phytother Res 36: 266-278, 2022.
32. Reyes-Farias M and Carrasco-Pozo C: The anti-cancer effect of quercetin: Molecular implications in cancer metabolism. Int J Mol Sci 20: 3177, 2019.
33. Wang B, Zhang W, Zhou X, Liu M, Hou X, Cheng Z and Chen D: Development of dual-targeted nano-dandelion based on an oligomeric hyaluronic acid polymer targeting tumor-associated macrophages for combination therapy of non-small cell lung cancer. Drug Deliv 26: 1265-1279, 2019.
34. Tang SM, Deng XT, Zhou J, Li QP, Ge XX and Miao L: Pharmacological basis and new insights of quercetin action in respect to its anti-cancer effects. Biomed Pharmacother 121: 109604, 2020.